Increase in liver γδ T cells with concurrent augmentation of IFN-β production during the early stages of a mouse model of acute experimental hepatitis B virus infection

LIN CHANG[1*], LEI WANG[2*], NING LING[3*], HUI PENG[4] and MIN CHEN[3]

[1]Department of Clinical Laboratory, People's Hospital of Bishan District, Chongqing 402760;
[2]Department of Clinical Laboratory, Taihe Hospital, Hubei University of Medicine, Shiyan, Hubei 442000;
[3]Key Laboratory of Molecular Biology for Infectious Diseases (Ministry of Education), Institute for Viral Hepatitis,
The Second Affiliated Hospital, Chongqing Medical University, Chongqing 400016; [4]Department of Clinical Laboratory,
The Second Affiliated Hospital, Chongqing Medical University, Chongqing 400010, P.R. China

Abstract. The role of γδ T cells in acute hepatitis B virus (HBV) infection remains unclear. For the present study, a mouse model of acute HBV infection was constructed using hydrodynamic injection-based transfection of an HBV DNA plasmid (pHBV). Subsequent changes in the percentages of γδ T cells, expression of activation molecules (CD25 and CD69) and the production of the inflammatory cytokines interferon (IFN)-γ and tumor necrosis factor-α (TNF-α) by liver γδ T cells were investigated using fluorescence-activated cell sorting (FACS). Additionally, the immune responses in the mouse liver were evaluated dynamically by measuring cytokine mRNA expression (IFN-α, IFN-β, IFN-γ or TNF-α) using reverse transcription-quantitative PCR, and other populations of immune cells, including CD4+T, CD8+T, natural killer (NK) or natural killer T (NKT) cells, using FACS. On day 1 following acute HBV infection, the percentage of liver γδ T cells was significantly increased along with the high expression of HBV markers. Additionally, liver γδ T cells displayed peak expression of the activation marker CD69 and peak IFN-γ production within this timeframe. IFN-β mRNA expression and the percentage of NK cells were elevated significantly on day 1 in liver tissues. However, there were no significant changes in the spleen or peripheral γδ T cells.

Correspondence to: Professor Min Chen, Key Laboratory of Molecular Biology for Infectious Diseases (Ministry of Education), Institute for Viral Hepatitis, The Second Affiliated Hospital, Chongqing Medical University, 1 Yixueyuan Road, Chongqing 400016, P.R. China
E-mail: mchen@hospital.cqmu.edu.cn

*Contributed equally

Therefore, these data suggested that during the early stages of acute HBV infection, significantly increased numbers of liver γδ T cells may be involved in the enhanced immune response to the increased expression of HBV markers in the liver.

Introduction

Hepatitis B virus (HBV) is a noncytopathic hepadnavirus that can lead to a wide spectrum of human liver diseases, ranging from acute to chronic hepatitis, cirrhosis and hepatocarcinoma (1). In total, ~10% of adults infected with HBV will develop chronic liver infection and it is estimated that 240 million people are chronic HBV carriers worldwide; ~650,000 people die each year due to complications of chronic hepatitis B (CHB) (2,3).

Understanding of the immunological events that take place in controlling HBV infection during its early phases has accelerated over recent years. Upon entering the body, the binding of the HBV pre-S1 region to the sodium taurocholate cotransporting polypeptide on hepatocytes elicits immediate HBV infection of the liver (4). After an incubation period of 4-10 weeks, hepatitis B surface antigen (HBsAg), hepatitis B e-antigen (HBeAg) or HBV DNA become detectable in the serum (1-3). The immune system can be activated in response to viral antigen expression or viral replication in infected hepatocytes. During the latter stages of infection, specific protective anti-HBV antibodies are produced, and memory T cells begin to develop, followed by the clearance of HBV infection. However, if the HBV infection is not adequately controlled during the acute stage of infection, chronic HBV infection can develop. Therefore, the immune response during this early stage is critical in determining the outcome of infection. However, the exact mechanism associated with this process remains unclear (5,6).

Understanding of the immunological mechanisms that occur during the early stages of HBV infection in the liver is limited due to the lack of a suitable model research. Nevertheless, some researchers have investigated these very early events using woodchuck (7), mouse (8) or chimpanzee (9)

models of acute HBV infection, with mouse models being the most widely used. The mouse model of acute HBV infection by hydrodynamic injection (HI) with an HBV supergenomic DNA construct was first developed by Yang *et al* (10). This immunocompetent model can be used to examine the hepatic immunological effectors required for HBV clearance. Previous studies using this model have suggested that cells or mediators associated with the innate immune response, including NK cells (11), toll-like receptors 2 (12) and iNOS (13), participate in the early response to HBV infection.

The innate immune system can respond very rapidly during the early or acute stages of infection to exert functions and boost the subsequent specific immunity. Compared with the extensively studied HBV-specific immunity, mechanisms of innate immune responses during the early stages of HBV infection remain to be defined (14-16).

γδ T cells, unlike conventional αβ T cells, express the γ and δ chains in their T cell receptors (TCRs). γδ T cells are a class of innate immune cells that share some functions with NK cells, including surface molecules (CD56 and killer cell lectin like receptor K1), production of cytokines [interferon (IFN)-γ and tumor necrosis factor-α (TNF-α)] and cytotoxic activity against infected or transformed cells (17). Indeed, the potential role of γδ T cells is garnering attention due to their reported participation in a plethora of immunological functions, including immune cytotoxicity, cytokine production, antigen presentation and immunological cross-talk with other cells (18,19). In murine cytomegalovirus or *Plasmodium falciparum* infection, γδ T cells are activated rapidly and initiate the secondary immune response (20,21). In HBV infection, previous studies have demonstrated reduced percentages of peripheral Vδ2 T cells in patients with CHB (22), whilst patients with asymptomatic, persistent HBV infection exhibit increased IFN-γ-producing γδ T cells (23). In a mouse model carrying HBV, γδ T cells have been shown to mobilize myeloid-derived suppressor cell (MDSC) infiltration into the liver, leading to MDSC-mediated CD8^{+} T cell exhaustion (24).

However, at present, the role of γδ T cells during acute HBV infection remains unclear. Therefore, the present study focused on assessing the changes that occur in the population of γδ T cells during acute HBV infection, especially in the liver, and whether they participate in the innate immune response during the early stages of HBV clearance. A mouse model of acute HBV infection was constructed using a hydrodynamics-based HBV plasmid transfection method reported previously (25,26). Using this immunocompetent mouse model, which mimics acute HBV infection, liver γδ T cells and innate immune responses in the liver tissue were dynamically observed. The results suggested that during the early stages of acute HBV infection, the percentage and function of liver γδ T cells was enhanced, which occurred concurrently with increased IFN-β expression and other innate immune responses in the liver.

Materials and methods

Mice, plasmids and HI. Female C57BL/6J mice (age, 4-6 weeks; weight range, 16-22 g) were purchased from the Animal Center of Chongqing Medical University (Chongqing, China). All animals were housed under specific pathogen-free conditions in which the ambient temperature (23±1˚C) and humidity (~35-45%) were controlled with a 12-h light/dark cycle and food and water *ad libitum* and treated according to the guidelines of the animal facility at the Chongqing Medical University. All experiments were approved by Chongqing Medical University and were conducted in accordance with the Guidelines for the Care and Use of Laboratory Animals in China (27).

An HBV replication-competent plasmid encoding the 1.3-fold overlength HBV genome [pcDNA3.1-HBV 1.3 (ayw subtype)] was a kind gift from Professor Ni Tang (Key Laboratory of Molecular Biology for Infectious Diseases, Institute for Viral Hepatitis, Chongqing Medical University, Chongqing, China). Corresponding control pcDNA3.1 vector was purchased from Invitrogen (Thermo Fisher Scientific, Inc.). All plasmids were reserved at -20˚C.

A total of 55 female mice were randomly divided into 11 groups, including 0 (normal mice), 1, 3, 5, 7 or 15 days after pHBV plasmid injection and 1, 3, 5, 7 or 15 days after control plasmid injection. Mice were then hydrodynamically injected with 15 µg plasmid dissolved in 1.5 ml saline solution through their tail veins within 5 sec. There were 5 mice per group in each experiment.

Peripheral blood, spleen and liver samples were collected for analysis at different timepoints following plasmid transfection. Mice were anesthetized by exposure to ether presented on a cotton ball inside a conical tube. A conical tube containing diethyl ether-soaked cotton balls was placed near the nose of each mouse without contact. The mice were fully anesthetized several minutes later, but remained alive with their hearts beating and body temperature kept constant at 37˚C. The mice were then fixed and placed in a supine position, the abdominal and thoracic cavities were subsequently opened and 0.5-0.8 ml blood samples were obtained from the heart, which were collected into a tube containing the anticoagulant EDTA. The portal vein was then perfused with 5 ml saline and the liver and spleen were collected in a plate filled with iced RPMI 1640 medium (Gibco; Thermo Fisher Scientific, Inc.) for cell and lymphocyte isolation. At the completion of the procedure, all mice were sacrificed by cervical dislocation prior to awakening from anesthesia. At the time of sacrifice, the weights of the mice had decreased to 15-19 g due to blood and tissue collection. No fixatives were applied during any of the aforementioned procedures.

Detection of serum HBV antigens, HBV DNA and liver function. On days 0, 1, 3, 5, 7 and 15 following transfection, levels of HBsAg and HBeAg in the serum were measured using cobas® HBsAg detection kit and cobas® HBeAg detection kit by electrochemiluminescence immunoassay (Roche Diagnostics) according to the manufacturer's protocols, with the results represented as cut-off index (COI) values. To avoid plasmid contamination, mouse serum was treated with 20 U DNAase I for ≥12 h, following which HBV DNA was extracted using a Viral DNA extraction kit (Da An Gene Co., Ltd., China), according to the manufacturer's protocol, and detected by reverse transcription-quantitative PCR (RT-qPCR) using a Roche Thermocycler (Roche Diagnostics) according to the manufacturer's protocol.

Within the same timeframe, alanine aminotransferase (ALT) levels were also measured in serum collected from the mice using a Hitachi 7600 Automatic Biochemical Analyzer (Hitachi, Ltd.).

Histology and immunohistochemical (IHC) staining for HBsAg and HBcAg expression in liver tissues. Liver histology was determined using hematoxylin-eosin (H&E) staining. Liver tissues ($6 \mu M$ sections) from pHBV-transfected mice on days 0, 1, 3, 5, 7 and 15 were fixed in 10% neutral formalin for 24 h at room temperature (RT), dehydrated using an ethanol gradient (70, 80, 90 and 100%) and embedded in paraffin. The slides were subsequently stained using H&E for 10 min at RT for histological examination.

IHC staining procedures were conducted according to the manufacturer's protocols. The main steps were as follows: Liver specimens ($6 \mu M$ sections) from pHBV-transfected mice on days 0, 1 and 5 were paraffin-embedded. Following de-paraffinization, rehydration using an ethanol gradient (95 and 80%) and antigen retrieval in a 0.1% trypsin solution at 37°C for 20 min, endogenous peroxidase was quenched using 3% H_2O_2 and unspecific binding was blocked using 2.5% goat serum (Cell Signaling Technology, Inc.) for 20 min at RT. Mouse anti-HBsAg primary monoclonal antibody (1:100, dilution; cat. no. ZM-0122) or mouse anti-HBcAg primary antibody (1:100, dilution; cat. no. ZM-0421; both ZSGB-BIO) was subsequently added, followed by incubation overnight at 4°C. The samples were then incubated with horseradish peroxidase-conjugated goat anti-mouse polymer (Elivision™ plus Polyer HRP (Mouse/Rabbit) IHC Kit; cat. no. KIT-9902) for 30 min at room temperature (Fuzhou Maixin Biotech Co., Ltd., China), followed by treatment with 3,3'-diaminobenzidine (DAB; Elivision Super; Fuzhou Maixin Biotech Co., Ltd., China). Yellow or brown dye in hepatocytes indicated positive staining. The percentage of positively stained cells were determined by counting in five random high-power fields using an Olympus optical light microscope (Olympus Corporation), where there were ≥100 cells in each field (magnification, x400).

Preparation of lymphocytes from the livers and spleens. Liver lymphocytes were isolated as previously reported (28). Briefly, mice were anaesthetized with diethyl ether and the portal vein was perfused with 5 ml saline until the liver became pale in color. The liver was then cut into small pieces, and incubated in RPMI 1640 solution (Gibco; Thermo Fisher Scientific, Inc.) supplemented with 0.05% collagenase IV (cat. no. C5138; Sigma-Aldrich; Merck KGaA) and 0.01% DNAase I (cat. no. D5025; Sigma-Aldrich; Merck KGaA) at 37°C for 30 min, after which the pieces were pressed through a 200-gauge stainless steel mesh. Following centrifugation at 50 x g (4°C, 10 min, the precipitate was discarded) and again at 500 x g (4°C, 10 min, the supernatant was discarded), the remaining cell pellet was resuspended in 3 ml RPMI-1640 solution (Gibco; Thermo Fisher Scientific, Inc.) and overlaid onto a 33% Percoll solution (cat. no. 17-0891-01; Pharmacia Biotech; GE Healthcare, USA), followed by centrifugation at 800 x g for 30 min at room temperature. The supernatant was then aspirated, and the red blood cells (RBC) were lysed using a 0.75% NH_4Cl solution. After subsequent washing with PBS, the liver lymphocytes were prepared for immediate FACS analysis.

Mouse spleen tissues were smashed and dissociated thoroughly using two glass slides with rough surfaces smeared beforehand with a RBC lysis buffer (0.75% NH_4Cl solution). After RBC lysis for 10 min, the cell suspension was filtered through a $70 \mu M$ filter (BD Biosciences) to obtain a single-cell suspension. The suspension was then washed with PBS and the lymphocyte-enriched spleen cells were prepared for later use.

Fluorescence-activated cell sorting (FACS) analysis of lymphocytes for cell surface markers and intracellular cytokine production. The following fluorochrome-conjugated mAbs were used according to the manufacturer's protocol: Purified anti-mouse CD16/CD32 (1:100 dilution; cat. no. 14-0161-81; eBioscience; Thermo Fisher Scientific, Inc.); peridinin-chlorophyll-protein complex-conjugated hamster anti-mouse CD3e (1:50 dilution; cat. no. 553067; BD Biosciences); phycoerythrin (PE)-conjugated hamster anti-mouse γδ TCR (1:50 dilution; cat. no. 553178; BD Biosciences); PE-Cy™7-conjugated anti-mouse CD69 (1:50 dilution; cat. no. 25-0691-81; eBioscience; Thermo Fisher Scientific, Inc.); allophycocyanin (APC)-conjugated rat anti-mouse CD25 (1:50 dilution; cat. no. 558643; BD Biosciences); fluorescein isothiocyanate (FITC)-conjugated hamster anti-mouse γδ TCR (1:100 dilution; cat. no. 553177; BD Biosciences); PE-conjugated anti-mouse IFN-γ (1:100 dilution; cat. no. 12-7311-81; eBioscience; Thermo Fisher Scientific, Inc.); PE-Cy™7-conjugated rat anti-mouse TNF-α (1:100 dilution; cat. no. 557644; BD Biosciences); PE-Cy™7 anti-mouse NK1.1 (1:50 dilution; cat. no. 552878; BD Biosciences); FITC-conjugated anti-mouse CD4 (1:100 dilution; cat. no. 553047; BD Biosciences); and APC-Cy™7-conjugated anti-mouse CD8 (1:50 dilution; cat. no. 557654; BD Biosciences).

For surface staining, liver lymphocytes (~$5x10^5$), splenic cells (~$5x10^5$) or 100 μl of fresh peripheral anticoagulated blood samples were used for staining. Cells were blocked using 0.5 μg anti-CD16/32 antibody for 10 min at 4°C, after which an appropriate volume of each specific antibody was added, and the samples were incubated for 30 min in the dark at 4°C. For whole-blood staining, erythrocytes were lysed using BD™ FACS™ lysing solution (BD Biosciences) and cells were washed using PBS supplemented with 1% fetal calf serum (FCS; Gibco; Thermo Fisher Scientific, Inc.).

Intracellular cytokine staining was performed as follows: Liver lymphocytes were adjusted to ~$5x10^6$ cells/ml in RPMI 1640 culture medium supplemented with 10% FCS and stimulated with 100 ng/ml phorbol myristate acetate plus 1 μg/ml ionomycin at 37°C for 4 h in the presence of the secretion inhibitor monensin (0.16 μg/ml; BD Biosciences) (29). Cells were blocked using 0.5 μg anti-CD16/32 antibody for 10 min at 4°C and then stained with anti-TCR γδ mAb for 30 min at 4°C, followed by washing with PBS and fixing in 4% paraformaldehyde. Stained cells were permeabilized using 0.1% saponin (Sigma-Aldrich; Merck KGaA) and incubated with anti-IFN-γ and anti-TNF-α for 30 min at 4°C.

Stained cells were immediately analyzed using the FACSCanto™ II flow cytometer (BD Immunocytometry Systems; BD Biosciences). Data were analyzed using FACSDiva™ 2.0 software (BD Immunocytometry Systems; BD Biosciences). Cell gating strategies were as follows: The population of cells double positive for γδ TCR and CD3 was

defined as the γδ T cell subtype, which was subsequently subdivided into several subsets, including CD25$^+$, CD69$^+$, IFN-γ$^+$ or TNF-α$^+$ γδ T cells, according to their positivity in the FACS dot plots. CD3 and NK1.1 were used to measure the presence of mouse NK and NKT cells; CD3- NK1.1+ cells were defined as NK cells (left upper quadrant) and CD3+ NK1.1+ cells were defined as NKT cells (right upper quadrant) (30).

RT-qPCR analysis for gene expression in the liver tissue. Liver tissue (~40 mg) in 1 ml TRIzol® solution (Invitrogen; Thermo Fisher Scientific, Inc.) was homogenized using a power homogenizer and the total RNA was extracted according to the manufacturer's protocols. RNA quality was evaluated by electrophoresis and spectral analysis. Only RNA without degradation or contamination with DNA or protein was used for subsequent RT-qPCR analyses.

RNA (~1 μg) was reverse transcribed by 2 min at 70°C, 15 min at 37°C, and then 1 min at 95°C with oligo (dT) primers using the PrimeScript™ RT Reagent kit with gDNA eraser, according to the manufacturer's protocol (Takara Bio, Inc.). qPCR was then performed using SYBR® Green quantitative PCR dye with SYBR® Premix Ex Taq™ II, according to the manufacturer's protocol (Takara Bio, Inc.). All samples were detected in triplicate using an Applied Biosystems 7300 Real-Time PCR Detection System (Applied Biosystems; Thermo Fisher Scientific, Inc.), according to the manufacturer's protocols. GAPDH was used as an internal control and the data were analyzed using the $2^{-\Delta\Delta Cq}$ method (31). Primer sequences for IFN-α, IFN-β, IFN-γ, TNF-α and GAPDH used for RT-qPCR are listed in Table I.

Statistical analysis. SPSS software (version 15.0; SPSS Inc.) was used to analyze all data. Experimental data are expressed as the mean ± SD, from five experimental repeats. Following one-way ANOVA, differences between every two groups were calculated using the Least Significant Difference method. For comparison of RNA expression, significant changes were assessed as at least a 2-fold increase or a 0.5-fold decrease. Pearson correlation analysis was performed to evaluate the correlation in the percentage of γδT cells with the relative fold changes in HBsAg or HBcAg RNA expression. P<0.05 was considered to indicate a statistically significant difference.

Results

Expression of HBV markers in serum and livers from mice with acute HBV infection. To verify that the mouse model of acute HBV infection was constructed successfully in the present study, serum HBsAg, HBeAg and HBV DNA levels and the intrahepatic expression of HBsAg and HBcAg were measured.

On day 1 after hydrodynamic-based pHBV plasmid injection, serum tested positive for HBsAg, HBeAg, and HBV DNA (Fig. 1A). HBV markers were undetectable in mice after control plasmid transfection (data not shown). After pHBV plasmid injection, HBsAg serum levels increased from 113.9±31.1 (COI) on day 1 to a peak value of 255.3±47.6 (COI) on day 3, followed by a decrease to 5.3±1.5 (COI) on day 15. Serum HBeAg levels were the highest on day 1 at 31.1±6.9 (COI) and then decreased gradually to 1.5±0.7 (COI) on day 15 (Fig. 1A). Additionally, the serum HBV DNA load

Table I. Sequences of primers used for reverse transcription-quantitative PCR.

Gene	Primer sequence
IFN-α (NM_010502)	F: 5'-GGATGTGACCTTCCTCAGACTC-3' R: 5'-ACCTTCTCCTGCGGGAATCCAA-3'
IFN-β (NM_010510)	F: 5'-GCCTTTGCCATCCAAGAGATGC-3' R: 5'-ACACTGTCTGCTGGTGGAGTTC-3'
IFN-γ (NM_008337)	F: 5'-CAGCAACAGCAAGGCGAAAAAG G-3' R: 5'-TTTCCGCTTCCTGAGGCTGGAT-3'
TNF-α (NM_013693)	F: 5'-GGTGCCTATGTCTCAGCCTCTT-3' R: 5'-GCCATAGAACTGATGAGAGGGA G-3'
HBsAg	F: 5'-GTGTCTGCGGCGTTTTATCA -3' R: 5'-GACAAACGGGCAACATACCTT-3'
HBcAg	F: 5'-TAGCTACCTGGGTGGGTGTT-3' R: 5'-AAGCTGGAGGAGTGCGAATC-3'
GAPDH	F: 5'-CATCACTGCCACCCAGAAGACT G-3' R: 5'-ATGCCAGTGAGCTTCCCGTTCA G-3'

IFN, interferon; TNF-α, tumor necrosis factor-α; HBsAg, hepatitis B surface antigen; HBcAg, hepatitis B core antigen; F, forward, R, reverse.

declined from an average of 3.2x10^4 copies/ml on day 1 to virtually undetectable levels on days 7 and 15 (Fig. 1A). In terms of liver function, serum ALT levels in pHBV-transfected groups increased on day 1 and then decreased back to normal levels (<30 U/l).

Liver histopathology was evaluated on days 0, 1, 3, 5, 7 and 15 after injection (Fig. 1B). An apparent accumulation of mononuclear cells was observed in the mouse livers on day 3. On day 5, the liver structure changed with the appearance of some necrotic lesions and hepatocyte degeneration. By day 7, the liver tissue recovered back to a normal architecture, which was also maintained on day 15 (Fig. 1B).

HBsAg and HBcAg expression was subsequently examined by immunohistochemistry with DAB staining in the liver specimens isolated from pHBV-transfected mice (Fig. 1C). The average percentages of positively stained cells were determined by counting in five random high-power fields. On day 1, an average of 13.8 or 11.2% hepatocytes were staining positive for HBsAg or HBcAg, respectively. HBsAg was mainly expressed in the cytoplasm, whilst HBcAg expression was observed in both the cytoplasm and the nucleus. However, HBsAg and HBcAg expression decreased sharply on day 5 post-injection, with only 0.6 and 1.2% of hepatocytes on average displaying positive expression of HBsAg and HBcAg, respectively (Fig. 1C).

Aside from HBsAg$^+$ or HBcAg$^+$ hepatocytes, HBsAg and HBcAg mRNA expression were also measured in the liver tissues using RT-qPCR, where the results also showed that HBV expression was increased at day 1 (Fig. S1).
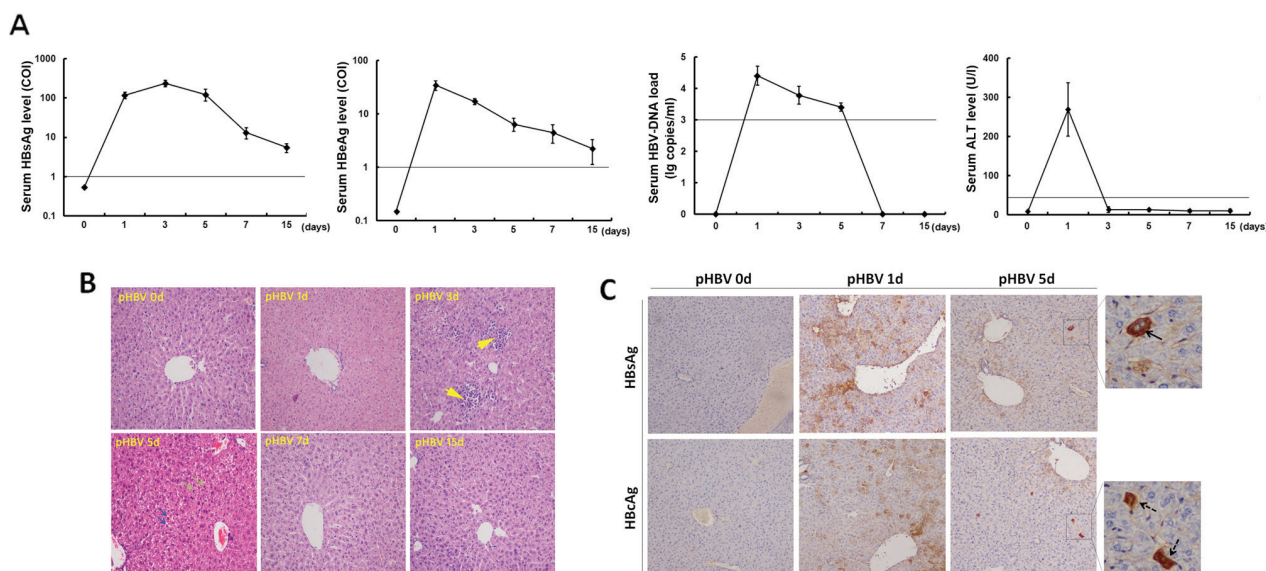
Figure 1. Assessment of acute HBV infection in mice following hydrodynamic transfection. Female C57BL/6J mice were transfected with the pcDNA3.1-HBV1.3 plasmid using the hydrodynamic method. (A) Serum levels of HBsAg, HBeAg, HBV DNA and ALT were detected on days 0, 1, 3, 5, 7 and 15 after pHBV plasmid injection. The straight lines in the graphs indicate the cut-off values. The HBV DNA load was displayed in a log 10 scale format. A total of five mice were used for each time point. Data at each time point are expressed as the mean ± SD. (B) Hematoxylin-eosin staining of liver specimens from pHBV-transfected mice on days 0, 1, 3, 5, 7 and 15. Yellow arrows indicated infiltrating mononuclear cells, and green or blue arrows indicated necrotic lesions or degeneration of hepatocytes, respectively. Magnification, x100. (C) HBsAg and HBcAg expression in murine liver tissue samples detected using immuno-histochemistry on days 0, 1 and 5 in pHBV-transfected mice. Arrows with solid or dashed lines show HBsAg- or HBcAg-positive hepatocytes, respectively. Magnification, x100 or x400. HBV, hepatitis B virus; HBeAg, hepatitis B virus e-antigen; HBsAg, hepatitis B surface antigen; pHBV, pcDNA3.1-HBV1.3 plasmid; ALT, alanine aminotransferase; COI, cut-off index.

Subsequent changes in liver γδ T cell percentages in mice following acute HBV infection. To investigate changes in γδ T cell numbers, the percentages of γδ T cells were first measured in the liver, spleen and peripheral blood samples of mice using FACS analysis, to dynamically monitor any changes following HBV plasmid injection (Fig. 2). Representative FACS dot plots for γδ T cells are shown in Fig. 2A. On day 0, the percentage of γδ T cells in the liver was 4.5±0.6% (percentage of total T cells), which was significantly higher compared with that observed in the spleen (2.1±0.3%; P<0.05) or the peripheral blood (1.2±0.6%; P<0.05). On day 1 post-injection, the percentage of liver γδ T cells increased to 8.3±2.9%, which was significantly higher compared with that on day 0 (4.5±0.6%; P<0.05) and that found in the liver samples of mice transfected with the control plasmid on day 1 (pcDNA; 3.8±0.7%; Fig. 2B). The percentage of liver γδ T cells in the pHBV-infected group gradually decreased to a level similar to that observed on day 0, while there were no significant changes in the percentage of liver γδ T cells after control plasmid transfection. Additionally, the percentages of spleen and blood γδ T cells from either the pHBV or pcDNA control groups displayed no significant changes compared with those on day 0 (P>0.05; Fig. 2C and D). In addition, the percentage of liver γδ T cells increased dramatically on day 1, which was in accordance with the highest percentage of HBsAg+ or HBcAg+ hepatocytes and the increased mRNA expression of HBsAg and HBcAg in the mouse livers (Fig. S1)

Activation of liver γδ T cells in pHBV-transfected mice. Following the observation that there was an increased percentage of total liver γδ T cells following pHBV transfection, the activation and function of these liver γδ T cells were investigated further by assessing the expression of CD25 and CD69, surface markers for activation (32) and intracellular cytokines IFN-γ and TNF-α (Fig. 3A). The percentages of CD25+ and CD69+ liver γδ T cells on day 0 were found to be 2.5±0.5 and 6.5±0.9% (of total γδ T cells), respectively (Fig. 3B and C). The percentage of CD69+ liver γδ T cells in the pHBV-transfected group increased to 18.9±4.7% on day 1 post-injection, which was significantly higher compared with that in the day 0 group (6.5±0.9%) or the pcDNA control group (7.7±1.8%) on day 1. CD69 expression declined to 8.7±1.6% on day 3 and settled to 9.6±1.5% on day 7. The percentage of CD25+ liver γδ T cells was found to be gradually elevated in the pHBV-transfected group, with an increase from 3.9±1.8% on day 1 to 7.1±2.1% on day 5, followed by a drop to 1.9±0.4% on day 7. The percentage of CD25+ γδ T cells on day 5 in pHBV-transfected group was significantly different when compared with the percentages on day 0 (2.5±0.5%) and in the pcDNA control on day 5 (3.2±0.9%; P<0.05). For the pcDNA control group, no significant differences were found in the percentages of either CD25+ or CD69+ γδ T cells across the different time points tested (P>0.05).

As shown in Fig. 3D and E, the percentages of IFN-γ- and TNF-α-producing liver γδ T cells were 5.1±0.4% and 4.7±0.6%, respectively, on day 0. After pHBV plasmid injection, the percentage of IFN-γ+ γδ T cells increased on day 1 (8.6±3.7%), but this difference was not significant when compared to the day 0 group (5.1±0.4%) or the pcDNA control group on day 1 (6.1±1.9%; P>0.05). The percentage then dropped to 5.4±0.5% on day 7. As for TNF-α-producing γδ T cells in the pHBV-transfected group, no significant changes were observed across all time points (P>0.05). There were also no significant differences in the percentages of IFN-γ+ or TNF-α+ γδ T cells
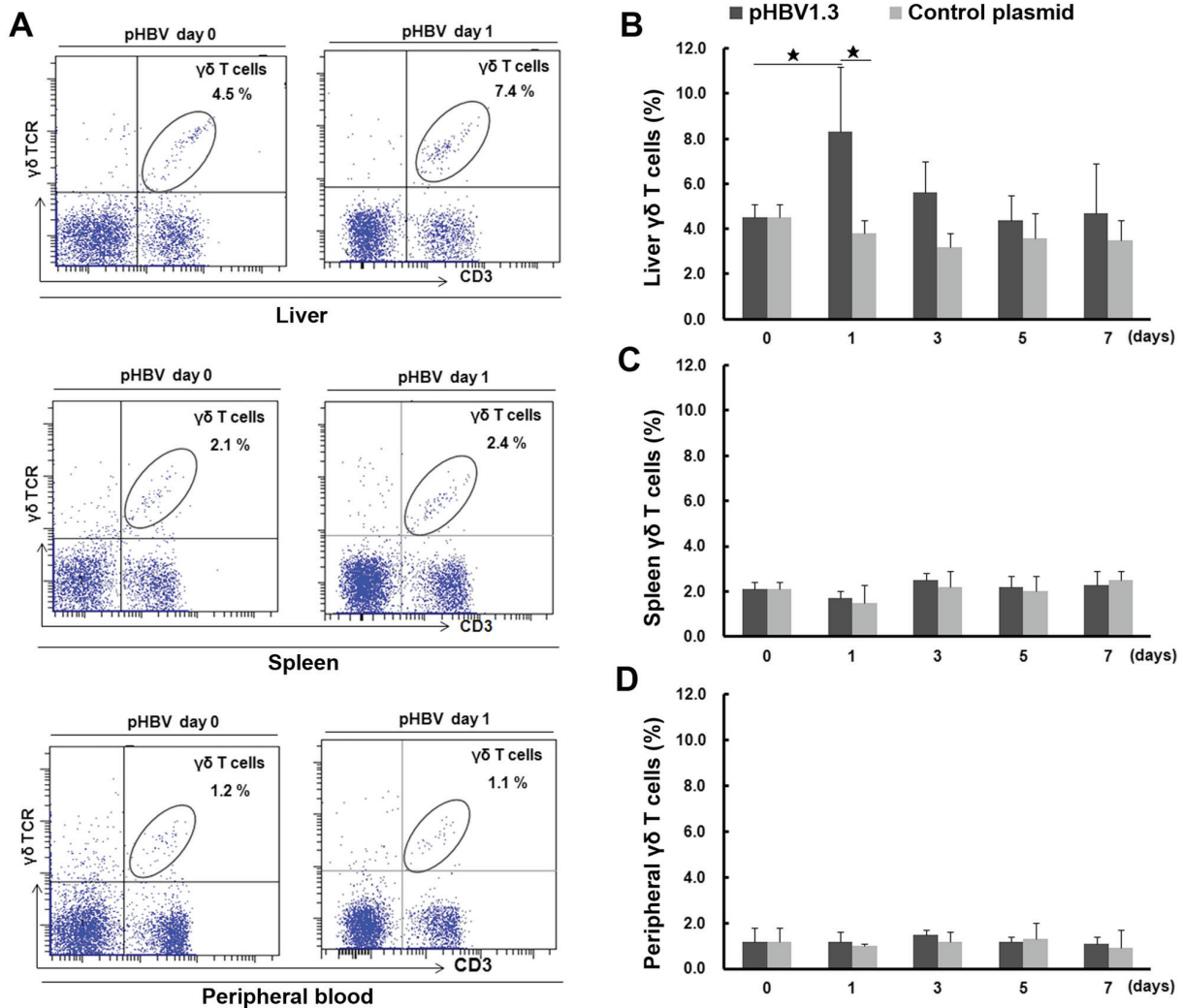
Figure 2. Percentage of γδ T cells in the liver, spleen and peripheral blood of pHBV- or control plasmid-transfected mice on days 0, 1, 3, 5 and 7. (A) The representative fluorescence-activated cell sorting plots show lymphocyte and γδ T cell populations in the liver, spleen and peripheral blood from pHBV mice at days 0 and 1 after plasmid transfection. The cell population in the right upper quadrant shows γδ T cells, and their percentages among the CD3$^+$ T cell populations are indicated in each panel. (B) The percentage of γδ T cells (% of total T cells) in the liver, (C) spleen and (D) peripheral blood at different time points after pHBV or control plasmid transfection. A total of five mice were used at each time point. Data at each time point are expressed as the mean ± SD. *P<0.05. γδTCR, γδ T cell receptor; HBV, hepatitis B virus; pHBV, pcDNA3.1-HBV1.3 plasmid.

compared with the pcDNA control group among all these time points (P>0.05).

Increased expression of IFN-β during the early phases of acute HBV infection. Since it was discovered that the number of liver γδ T cells from mice with acute HBV infection was increased, the possibility that other innate immune responses were activated in the liver was next explored. Early cytokine production is the most important activity associated with the antiviral innate immune response (33). Therefore, the mRNA expression of cytokine markers associated with the activation of the innate immune response, IFN-α and IFN-β, in addition to IFN-γ and TNF-α, were measured in liver tissues on days 0, 1, 3, 5 and 7 following injection with pHBV or the control plasmid. After pHBV injection, IFN-β mRNA expression was significantly upregulated, by an average of 6.8-fold on day 1 and by 2.5-fold on day 3 compared with that on day 0. It was also significantly higher compared with that in mice injected with the control pcDNA plasmid on days 1 (8.4-fold) and 3 (2.8-fold).

IFN-β expression subsequently decreased to normal levels on days 5 and 7. No significant changes in IFN-β expression were observed in the pcDNA control group. TNF-α expression in tissues from the pHBV-transfected group was increased slightly on day 1 (1.9-fold) compared with day 0, but no significant difference was observed in IFN-α or IFN-γ mRNA expression between pHBV-transfected or control groups across all time points examined (Fig. 4).

Changes in CD4$^+$ T, CD8$^+$ T, NK and NK T cell populations from mice with acute HBV infection. FACS dot plots of liver CD4$^+$ T, CD8$^+$ T, NK and NK T cells are shown in Fig. 5A. The percentage of liver NK cells from the pHBV-transfected group on day 1 was significantly higher compared with that in the control group (Fig. 5D). No significant differences were found in the percentages of CD4$^+$ T, CD8$^+$ T or NK T cells between the pHBV-transfected and control groups (Fig. 5B, C and E). Notably, the percentage of liver NK T cells decreased on day 3 compared with day 0 after plasmid injection in either the pHBV
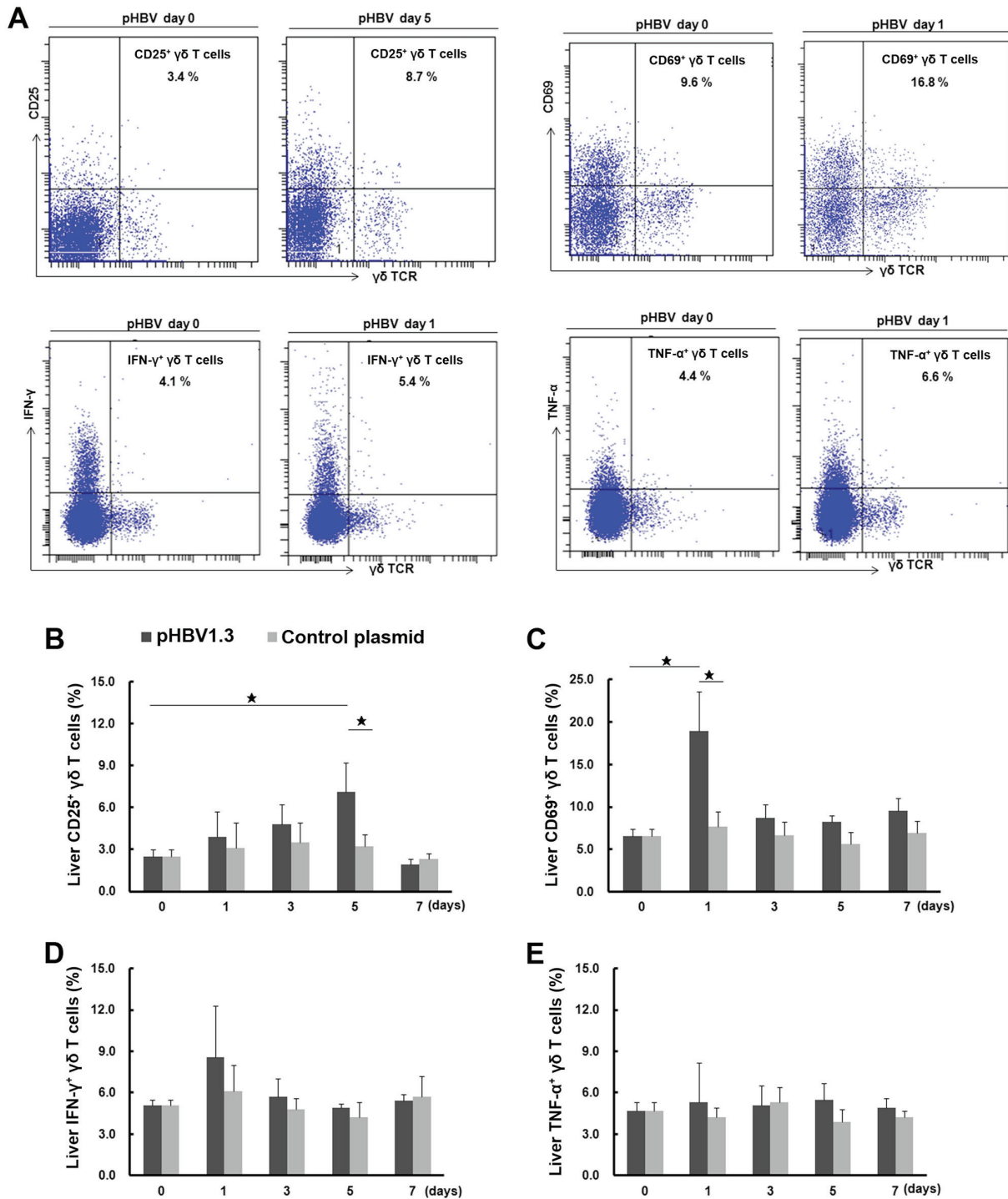
Figure 3. Activation of liver γδ T cells after pHBV plasmid transfection. (A) Representative FACS dot plots showing the expression of CD25, CD69, IFN-γ and TNF-α in liver γδ T cells from mice transfected with pHBV on days 0 and 1 or 5 after plasmid transfection. The cell population in the right upper quadrant showed CD25$^+$, CD69$^+$, IFN-γ$^+$ or TNF-α$^+$ γδ T cells and their respective percentages among total γδ T cells as indicated in the figures. (B) Dynamic changes in the percentage of CD25$^+$, (C) CD69$^+$, (D) IFN-γ$^+$ and (E) TNF-α$^+$ liver γδ T cells on days 0, 1, 3, 5 and 7 after transfection with the pHBV1.3 or control plasmid. A total of five mice were used at each time point. Data at each time point are expressed as the mean ± SD. *P<0.05. γδTCR, γδ T cell receptor; HBV, hepatitis B virus; pHBV, pcDNA3.1-HBV1.3 plasmid; IFN-γ, interferon-γ; TNF-α, tumor necrosis factor-α.

or pcDNA control groups, but the observed differences were not significant (Fig. 5E).

Discussion

It has been unclear what the exact mechanism of HBV clearance is in the early phases of infection (34,35). In early previous

studies, CD8$^+$ T cells were reported as the key cellular mediator of HBV clearance from the liver (3,5,6,11). Activated and polyclonal HBV-specific CD8$^+$ T cells can always be detected during the recovery of HBV-infected patients, whereas weakly activated and oligoclonal T cells are generally associated with persistent HBV infections (36). However, there were some recent reports demonstrating that the innate immune
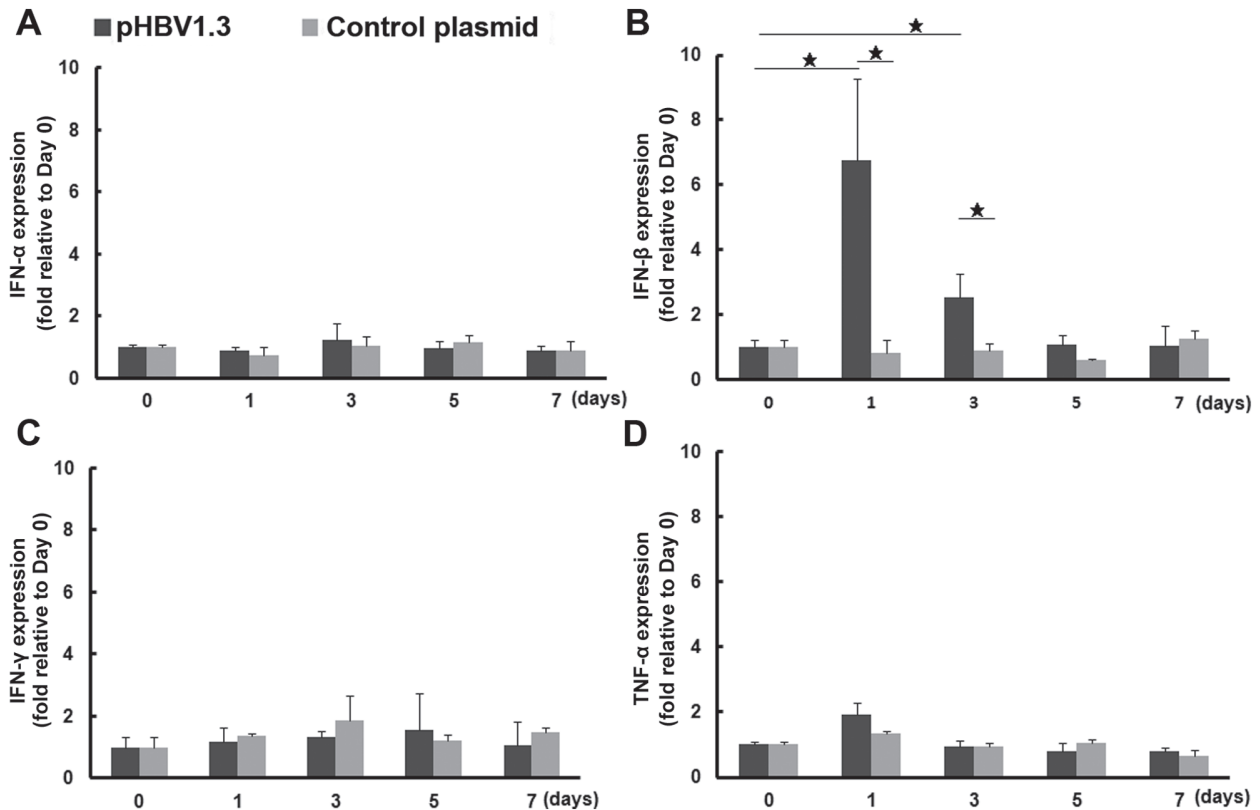
Figure 4. Cytokine mRNA expression in the livers of mice following acute HBV infection. Total mRNA was extracted from mouse liver specimens on days 0, 1, 3, 5 and 7 after transfection with pHBV1.3 or control plasmid. (A) Relative mRNA expression (fold change over day 0) of IFN-α, (B) IFN-β, (C) IFN-γ, and (D) TNF-α. A total of five mice were used at each time point. Data at each time point are expressed as the mean ± SD. *P<0.05. IFN, interferon; HBV, hepatitis B virus; pHBV, pcDNA3.1-HBV1.3 plasmid.

response serves important roles in the early stages of HBV infection (37,38). Although γδ T cells are innate immune cells with multifaceted functions, including antigen presentation, cytotoxicity, and cytokine production (39-41), the role of this cell type in the mechanism of HBV clearance during the early stages of infection remains unclear.

In the present study, to observe changes in innate immune responses and γδ T cells during the acute stage of HBV infection, specifically in the liver, a mouse model of acute HBV infection was successfully constructed, evidenced by the mouse serum and liver samples testing positive for HBV markers on day 1 and then mostly eliminated 15 days after pHBV plasmid injection. Previous studies have also shown that HBV can replicate in the liver of this mouse model (10,13,25). Differences in mouse strains, plasmids/vectors or plasmid quality can result in different levels of HBV marker expression in different mouse models (25). Using the mouse model established in the present study, the apparent infiltration of inflammatory cells into the liver was observed, in addition to increased ALT levels in the pHBV-transfected group compared with the pcDNA control group. This suggested that this mouse model of HBV infection may involve liver inflammation and injury.

The observation of positive correlation between the percentage of γδ T cells and expression of HBsAg or HBcAg in liver on day 1, suggesting that γδ T cells responded rapidly to HBV expression in the early stages of infection. In contrast, during the course of HBV expression, different expression patterns of CD69 and CD25 or inflammatory cytokines IFN-γ

and TNF-α were found on γδ T cells, suggesting that these subtypes may carry different functions. Indeed, in previous studies where comparisons in the function of IFN-γ- or TNF-α- producing T cells were conducted, HBV-specific TNF-α producing CD4 T cells was found to be associated with liver damage, whereas HBV-specific IFN-γ producing CD4 T cells was more associated with viral clearance in chronic HBV infection patients (42). This is in contrast with another study, where TNF-α production by γδ T cells was not as crucial as IFN-γ in the pathogenesis of experimental autoimmune encephalomyelitis (43).

The initiation of immune responses was next assessed in the mouse model of acute HBV infection from the present study. IFN-β is the most important cytokine associated with antiviral innate responses in host cells (44). When viruses enter a host cell, viral DNA or RNA is recognized by intracellular receptors or sensors which can induce the expression of type I IFNs, especially that of IFN-β (45). Meanwhile, the NF-κB pathway is activated, which is followed by an increase in the expression of inflammatory cytokines such as TNF-α (44,45). In the present study, the expression of IFN-β and TNF-α were elevated on day 1 in pHBV-transfected mice, which may be associated with the immune response to HBV infection. Both IFN-β and IFN-α are type I IFNs; however, unlike IFN-β, IFN-α expression was not significantly increased in the model from the present study. This difference may be the result of differential mechanisms in IFN-α and IFN-β production. IFN-γ has been previously reported to be the key immune
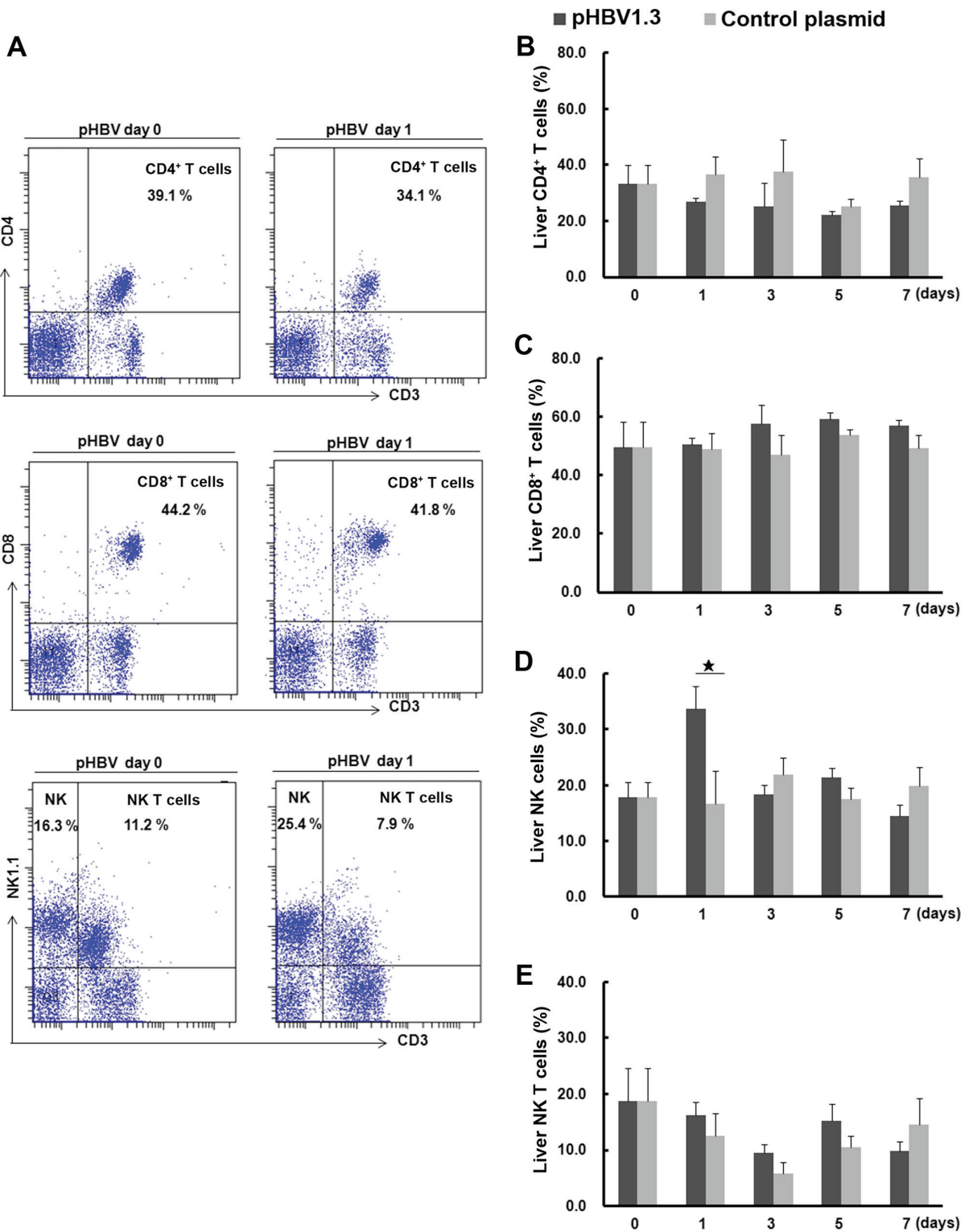
Figure 5. Percentages of liver CD4+ T, CD8+ T, NK or NKT cells in mice following acute HBV infection. (A) Representative fluorescence-activated cell sorting dot plots of CD4+ T, CD8+ T, NK and NKT cells in mouse liver samples on days 0 and 1 after pHBV or control plasmid transfection. The percentages of CD4+ T and CD8+ T cells among CD3+ T cells, or NK and NKT cells among all lymphocytes gated by FSC and side scatter SSC are indicated. (B) Changes in the percentages of CD4+ and (C) CD8+ T cells, (D) NK and (E) NKT cells on days 0, 1, 3, 5 and 7 after pHBV1.3 or control plasmid transfection. A total of five mice were used at each time point. Data at each time point are expressed as the mean ± SD. *P<0.05. NK, natural killer; HBV, hepatitis B virus; pHBV, pcDNA3.1-HBV1.3 plasmid; FSC, forward scatter; SSC, side scatter.

factor for HBV clearance in chimpanzee models of acute HBV infection (46). However, in the present study, IFN-γ mRNA expression did not show any significant changes in the pHBV-transfected group.

Changes in the numbers of γδ T cells of patients with other viral hepatitis infections have been previously observed. A study by Tseng et al (47) showed that liver biopsy specimens of hepatitis C virus (HCV)-infected patients contained high

numbers of γδ T cells, with high levels of non-major histocompatibility complex-restricted cytotoxic activity, and IFN-γ and TNF-α production, demonstrating that γδ T cells may serve a role in the pathology of HCV infections. In another study by Abravanel *et al* (48), increased CD69 expression was exhibited by γδ cells during the acute phase of hepatitis E virus (HEV) infection in patients with a solid-organ transplant, but this change was not associated with HEV clearance. In another study by Wu *et al* (49), activated liver γδT cells were found to be cytotoxic towards hepatocytes infected with murine hepatitis virus strain 3 (MHV-3), which may have contributed to the pathogenesis of MHV-3-induced murine fulminant viral hepatitis. In the present study, increased liver γδ T cells were found to be associated with the elimination of acute HBV infection. The aforementioned data suggest that changes in γδ T cell levels appear to be common in infections with hepatitis viruses, including HBV, HCV and HEV. However, this change in γδ T cell number may serve different roles in a manner that is dependent on the type of infection.

In a previous study by Kong *et al* (24), an HBV immunotolerant (HBV carrier) mouse model was constructed by injection of a relatively low amount (6 μg) of AAV/HBV1.2 plasmid. This mouse model was characterized by persistent HBV expression in the liver for >6 months, which was used to mimic the process of chronic HBV infection with immunotolerant status. Using this model, Kong *et al* found that γδT cells served a regulatory role in liver tolerance by inducing MDSC-mediated CD8+ T cell exhaustion. In another study, Li *et al* (26) observed HBsAg expression and immune responses in a C57/BL6 or BALB/c HBV infection mouse model mediated by pAAV-HBV HI of different doses of plasmids. In this model, high plasmid doses (10 or 100 μg) resulted in rapid HBV clearance and stronger immune responses, and HBV persistence for >6 months tended to occur at higher frequencies in C57/BL6 mice. In the present study, an acute HBV infection mouse model was constructed by injecting a relatively high amount (15 μg) of pcDNA3.1/HBV1.3 plasmid. Serum HBV DNA was negative at day 7 after plasmid injection, which suggests that the clearance of HBV occurred in this mouse model. In addition, the present study showed that γδ T cells may contribute to HBV clearance in this model. Therefore, γδT cells may serve different roles at different stages of HBV infection.

The roles of NK cells in acute hepatitis B infection have been extensively studied in mice and humans. Early and rapid activation of NK cells has been reported to contribute to HBV clearance, where their dysfunction was associated with the persistence of HBV infection (14). γδT cells are innate immune cells that are not dissimilar to NK cells, which share some common characteristics with regards to virus clearance, including the expression of cytotoxic molecules, including granzyme and perforin, or the production of inflammatory cytokines, including IFN-γ and TNF-α (17). In the present study, γδ T and NK cells were found to be enhanced at 1 day after pHBV injection, implying that these two populations of immune cells exert some common functions during the process of acute HBV infection and/or subsequent HBV clearance.

Although the contribution of the innate immune response during the early stages of HBV infection remains to be clearly defined (6), it has been previously shown to be involved in HBV clearance in a mouse model (11), a woodchuck model (7) and human hepatocyte cell lines (50). These aforementioned studies found that expression of type I IFN, IL-6 and chemokine CXCL10 are enhanced shortly after HBV infection and are involved in HBV clearance. Similar to these studies, the present study also showed that the levels of the intrahepatic cytokine IFN-β increased during the early stages of infection, which coincided with the increased expression of HBV DNA and antigens. Compared with the peripheral blood or spleen, NK, NKT or γδT cells are more abundant in liver, where they may rapidly respond to stimuli (51). Therefore, immediately after HBV expression and type I IFN production, the intrahepatic γδ T cells are activated very quickly; no significant changes in the percentage of γδ T cells were found in peripheral blood or spleen in the present study.

The lack of HCV or HAV inclusion is a possible limitation to the present study. In addition, changes in γδT cell populations at timepoints earlier than 1 day, and analysis of the correlation between γδT cells and liver HBsAg and HBcAg mRNA expression at each timepoint beyond 1 day, are required in further experiments.

In conclusion, taking all of these results into consideration, data from the present study indicated that immediately after HBV expression in the mouse liver, the percentage of γδ T cells increased along with their enhanced function. These observations were accompanied by the activation of immune responses, including increased IFN-β expression. Therefore, liver γδ T cells may be involved in the early innate immune response to HBV infection, which may provide a new clue to elucidating the mechanism of viral clearance during the acute stages of HBV infection.

Acknowledgements

Funding

Availability of data and materials

The data used and/or analyzed during the current study are available from the corresponding author on reasonable request.

Authors' contributions

MC designed and supervised this research. LC, LW, NL and HP performed the animal experiments, detected all indices, analyzed the data and wrote manuscript. All authors read and approved the final manuscript.

Ethics approval and consent to participate

This study was approved by the Ethics Committee of Chongqing Medical University (Chongqing, China)

Patient consent for publication

Not applicable.

Competing interests

The author declare that they have no competing interests.

References

1. Seto WK, Lo YR, Pawlotsky JM and Yuen MF: Chronic hepatitis B virus infection. Lancet 392: 2313-2324, 2018.
2. Tang LSY, Covert E, Wilson E and Kottilil S: Chronic hepatitis B infection: A review. JAMA 319: 1802-1813, 2018.
3. Tsai KN, Kuo CF and Ou JJ: Mechanisms of hepatitis B virus persistence. Trends Microbiol 26: 33-42, 2018.
4. Yan H, Zhong G, Xu G, He W, Jing Z, Gao Z, Huang Y, Qi Y, Peng B, Wang H, et al: Sodium taurocholate cotransporting polypeptide is a functional receptor for human hepatitis B and D virus. Elife 1: e00049, 2012.
5. Chang JJ and Lewin SR: Immunopathogenesis of hepatitis B virus infection. Immunol Cell Biol 85: 16-23, 2007.
6. Gehring AJ and Protzer U: Targeting innate and adaptive immune responses to cure chronic HBV infection. Gastroenterology 156: 325-337, 2019.
7. Guy CS, Mulrooney-Cousins PM, Churchill ND and Michalak TI: Intrahepatic expression of genes affiliated with innate and adaptive immune responses immediately after invasion and during acute infection with woodchuck hepadnavirus. J Virol 82: 8579-8591, 2008.
8. Stevens KE, Thio CL and Osburn WO: CCR5 deficiency enhances hepatic innate immune cell recruitment and inflammation in a murine model of acute hepatitis B infection. Immunol Cell Biol 97: 317-325, 2019.
9. Murray JM, Wieland SF, Purcell RH and Chisari FV: Dynamics of hepatitis B virus clearance in chimpanzees. Proc Natl Acad Sci USA 102: 17780-17785, 2005.
10. Yang PL, Althage A, Chung J and Chisari FV: Hydrodynamic injection of viral DNA: A mouse model of acute hepatitis B virus infection. Proc Natl Acad Sci USA 99: 13825-13830, 2002.
11. Yang PL, Althage A, Chung J, Maier H, Wieland S, Isogawa M and Chisari FV: Immune effectors required for hepatitis B virus clearance. Proc Natl Acad Sci USA 107: 798-802, 2010.
12. Lin Y, Huang X, Wu J, Liu J, Chen M, Ma Z, Zhang E, Liu Y, Huang S, Li Q, et al: Pre-activation of toll-like receptor 2 enhances CD8$^+$ T-cell responses and accelerates hepatitis B virus clearance in the mouse models. Front Immunol 9: 1495, 2018.
13. Chang WW, Su IJ, Lai MD, Chang WT, Huang W and Lei HY: The role of inducible nitric oxide synthase in a murine acute hepatitis B virus (HBV) infection model induced by hydrodynamics-based in vivo transfection of HBV-DNA. J Hepatol 39: 834-842, 2003.
14. Golsaz-Shirazi F, Amiri MM and Shokri F: Immune function of plasmacytoid dendritic cells, natural killer cells, and their crosstalk in HBV infection. Rev Med Virol 28: e2007, 2018.
15. Peeridogaheh H, Meshkat Z, Habibzadeh S, Arzanlou M, Shahi JM, Rostami S, Gerayli S and Teimourpour R: Current concepts on immunopathogenesis of hepatitis B virus infection. Virus Res 245: 29-43, 2018.
16. Fisicaro P, Valdatta C, Boni C, Massari M, Mori C, Zerbini A, Orlandini A, Sacchelli L, Missale G and Ferrari C: Early kinetics of innate and adaptive immune responses during hepatitis B virus infection. Gut 58: 974-982, 2009.
17. Lawand M, Déchanet-Merville J and Dieu-Nosjean MC: Key features of gamma-delta T-cell subsets in human diseases and their immunotherapeutic implications. Front Immunol 8: 761, 2017.
18. Kabelitz D and Déchanet-Merville J: Editorial: 'Recent advances in gamma/delta T cell biology: New ligands, new functions, and new translational perspectives'. Front Immunol 6: 371, 2015.
19. Rajoriya N, Fergusson JR, Leithead JA and Klenerman P: Gamma delta T-lymphocytes in hepatitis C and chronic liver disease. Front Immunol 5: 400, 2014.
20. Khairallah C, Netzer S, Villacreces A, Juzan M, Rousseau B, Dulanto S, Giese A, Costet P, Praloran V, Moreau JF, et al: γδ T cells confer protection against murine cytomegalovirus (MCMV). PLoS Pathog 11: e1004702, 2015.
21. Howard J, Zaidi I, Loizon S, Mercereau-Puijalon O, Déchanet-Merville J and Mamani-Matsuda M: Human Vγ9Vδ2 T Lymphocytes in the Immune Response to *P. falciparum* Infection. Front Immunol 9: 2760, 2018.
22. Chen M, Zhang D, Zhen W, Shi Q, Liu Y, Ling N, Peng M, Tang K, Hu P, Hu H and Ren H: Characteristics of circulating T cell receptor gamma-delta T cells from individuals chronically infected with hepatitis B virus (HBV): An association between V(delta)2 subtype and chronic HBV infection. J Infect Dis 198: 1643-1650, 2008.
23. Conroy MJ, Mac Nicholas R, Taylor M, O'Dea S, Mulcahy F, Norris S and Doherty DG: Increased frequencies of circulating IFN-γ-producing Vδ1(+) and Vδ2(+) γδ T cells in patients with asymptomatic persistent hepatitis B virus infection. Viral Immunol 28: 201-208, 2015.
24. Kong X, Sun R, Chen Y, Wei H and Tian Z: γδT cells drive myeloid-derived suppressor cell-mediated CD8+ T cell exhaustion in hepatitis B virus-induced immunotolerance. J Immunol 193: 1645-1653, 2014.
25. Huang M, Sun R, Huang Q and Tian Z: Technical improvement and application of hydrodynamic gene delivery in study of liver diseases. Front Pharmacol 8: 591, 2017.
26. Li L, Li S, Zhou Y, Yang L, Zhou D, Yang Y, Lu M, Yang D and Song J: The dose of HBV genome contained plasmid has a great impact on HBV persistence in hydrodynamic injection mouse model. Virol J 14: 205, 2017.
27. China National Standardization Administration: Guidelines for the Care and Use of Laboratory Animals in China, http://www.gb688.cn/bzgk/gb/newGbInfo?hcno=9BA619057D5C13103622A10FF4BA5D14. Accessed February 6, 2018.
28. Duwaerts CC, Sun EP, Cheng CW, van Rooijen N and Gregory SH: Cross-activating invariant NKT cells and kupffer cells suppress cholestatic liver injury in a mouse model of biliary obstruction. PLoS One 8: e79702, 2013.
29. Zhang H, Fu R, Guo C, Huang Y, Wang H, Wang S, Zhao J and Yang N: Anti-dsDNA antibodies bind to TLR4 and activate NLRP3 inflammasome in lupus monocytes/macrophages. J Transl Med 14: 156, 2016.
30. Li L, Cha H, Yu X, Xie H, Wu C, Dong N and Huang J: The characteristics of NK cells in Schistosoma japonicum-infected mouse spleens. Parasitol Res 114: 4371-4379, 2015.
31. Livak KJ and Schmittgen TD: Analysis of relative gene expression data using real-time quantitative PCR and the 2(-Delta Delta C(T)) method. Methods 25: 402-408, 2001.
32. Inatsuka C, Yang Y, Gad E, Rastetter L, Disis ML and Lu H: Gamma delta T cells are activated by polysaccharide K (PSK) and contribute to the anti-tumor effect of PSK. Cancer Immunol Immunother 62: 1335-1345, 2013.
33. Melchjorsen J: Learning from the messengers: Innate sensing of viruses and cytokine regulation of immunity-clues for treatments and vaccines. Viruses 5: 470-527, 2013.
34. Nosratabadi R, Alavian SM, Zare-Bidaki M, Shahrokhi VM and Arababadi MK: Innate immunity related pathogen recognition receptors and chronic hepatitis B infection. Mol Immunol 90: 64-73, 2017.
35. Tzeng HT, Tsai HF, Chyuan IT, Liao HJ, Chen CJ, Chen PJ and Hsu PN: Tumor necrosis factor-alpha induced by hepatitis B virus core mediating the immune response for hepatitis B viral clearance in mice model. PLoS One 9: e103008, 2014.
36. Boni C, Fisicaro P, Valdatta C, Amadei B, Di Vincenzo P, Giuberti T, Laccabue D, Zerbini A, Cavalli A, Missale G, et al: Characterization of hepatitis B virus (HBV)-specific T-cell dysfunction in chronic HBV infection. J Virol 81: 4215-4225, 2007.
37. Bertoletti A and Ferrari C: Adaptive immunity in HBV infection. J Hepatol 64 (1 Suppl): S71-S83, 2016.
38. Yoshio S and Kanto T: Host-virus interactions in hepatitis B and hepatitis C infection. J Gastroenterol 51: 409-420, 2016.
39. Deniger DC, Moyes JS and Cooper LJ: Clinical applications of gamma delta T cells with multivalent immunity. Front Immunol 5: 636, 2014.
40. Wu YL, Ding YP, Tanaka Y, Shen LW, Wei CH, Minato N and Zhang W: γδ T cells and their potential for immunotherapy. Int J Biol Sci 10: 119-135, 2014.

41. Paul S and Lal G: Regulatory and effector functions of gamma-delta (γδ) T cells and their therapeutic potential in adoptive cellular therapy for cancer. Int J Cancer 139: 976-985, 2016.
42. Wang H, Luo H, Wan X, Fu X, Mao Q, Xiang X, Zhou Y, He W, Zhang J, Guo Y, *et al*: TNF-α/IFN-γ profile of HBV-specific CD4 T cells is associated with liver damage and viral clearance in chronic HBV infection. J Hepatol: Sep 6, 2019 (Epub ahead of print).
43. Wohler JE, Smith SS, Zinn KR, Bullard DC and Barnum SR: Gammadelta T cells in EAE: Early trafficking events and cytokine requirements. Eur J Immunol 39: 1516-1526, 2009.
44. Ma Z, Ni G and Damania B: Innate sensing of DNA virus genomes. Annu Rev Virol 5: 341-362, 2018.
45. Brubaker SW, Bonham KS, Zanoni I and Kagan JC: Innate immune pattern recognition: A cell biological perspective. Annu Rev Immunol 33: 257-290, 2015.
46. Wieland S, Thimme R, Purcell RH and Chisari FV: Genomic analysis of the host response to hepatitis B virus infection. Proc Natl Acad Sci USA 101: 6669-6674, 2004.
47. Tseng CT, Miskovsky E, Houghton M and Klimpel GR: Characterization of liver T-cell receptor gammadelta T cells obtained from individuals chronically infected with hepatitis C virus (HCV): Evidence for these T cells playing a role in the liver pathology associated with HCV infections. Hepatology 33: 1312-1320, 2001.
48. Abravanel F, Barragué H, Dörr G, Sauné K, Péron JM, Alric L, Kamar N, Izopet J and Champagne E: Conventional and innate lymphocytes response at the acute phase of HEV infection in transplanted patients. J Infect 72: 723-730, 2016.
49. Wu D, Yan WM, Wang HW, Huang D, Luo XP and Ning Q: γδ T cells contribute to the outcome of murine fulminant viral hepatitis via effector cytokines TNF-α and IFN-γ. Curr Med Sci 38: 648-655, 2018.
50. Yoneda M, Hyun J, Jakubski S, Saito S, Nakajima A, Schiff ER and Thomas E: Hepatitis B virus and DNA stimulation trigger a rapid innate immune response through NF-κB. J Immunol 197: 630-643, 2016.
51. Heymann F and Tacke F: Immunology in the liver-from homeostasis to disease. Nat Rev Gastroenterol Hepatol 13: 88-110, 2016.